

Spatially Interpolated OFDM with Channel Estimation for Fast Fading Channels

Peter Klenner and Karl-Dirk Kammeyer

University of Bremen, Department of Communications Engineering
28359 Bremen, Germany

Email: {klenner,kammeyer}@ant.uni-bremen.de

Abstract—OFDM is well suited for data-transmission over frequency-selective channels. If the cyclic prefix is chosen sufficiently long, intersymbol interference is avoided. Thus, the linear convolution becomes circular and the channel is rendered into a set of flat-fading channels, which can be easily equalized. But this holds no longer in the case of large Doppler spread, i.e., when the channel is rapidly changing. Then the subcarriers lose their orthogonality giving rise for so-called intercarrier interference which is detrimental for the overall system performance. Among previous proposals to cope with this problem was the use of multiple receive antennas. These are positioned in the moving direction of the receiver such that the individual antennas are receiving delayed replica of the transmit signal via identical paths. By means of interpolation this enables to fabric a virtual non moving point of reception which seemingly experiences no Doppler spread. So far, this technique has been applied in a purely noncoherent setting resorting to differential modulation. We will demonstrate how this approach can be exploited by coherent reception. Our emphasis thereby lies on the use of higher-level modulation as well as Least-Square (LS) and Minimum Mean Square Error (MMSE) channel estimation.

I. INTRODUCTION

Orthogonal Frequency Division Multiplexing (OFDM) has been specifically designed for coping with multipath fading. Assuming that the impulse response of the channel is not exceeding the cyclic prefix as well as staying almost constant during the OFDM symbol duration, the channel matrix becomes circulant and is diagonalized by the IDFT/DFT matrix. However, a rapidly changing channel with large Doppler spread will violate this property. This is due to the Dirichlet subcarrier spectra which are broadened such that the subcarriers are no longer orthogonal. Equivalently, the channel matrix in frequency domain is no longer diagonal and exhibits significant off-diagonal elements.

The major difficulty arises in connection with channel estimation. Not only the data symbols, but also the pilot symbols within the OFDM time-frequency grid are impaired by the resulting intercarrier interference (ICI). Hence, the estimate of the channel will be corrupted leading to an unsatisfying data detection.

Conventional approaches to deal with ICI are based on reconstructing the channel's impulse response, e.g. [1], [2]. This technique basically performs an initial channel estimation based on the ICI-corrupted pilot symbols, upon which the channel matrix is reconstructed assuming a linear model for the channel variations. The shortcomings of this technique

are the limited range of Doppler spreads for which the linear model is valid and the increased computational demand, i.e., matrix inversion becomes necessary.

The weak spot of this solution is that it admits ICI in the first place, thus, allowing for the ICI to corrupt the pilots leading to a degraded channel estimation. The authors of [3], [4] tackle the problem by employing multiple receive antennas and a pre-processing of the received OFDM signal in time-domain prior to the FFT. The idea is to position the antennas in the direction of the motion, such that the individual antennas will see identical paths with a delay which is determined by their distance. With these receive signals at hand one can design a Wiener/MMSE interpolator which generates a virtual, non moving receive antenna, i.e., seemingly the pre-processed signal will have been received via a channel with a constant impulse response. Remarkable results are presented in [3], [4] proving the effectiveness of this approach, however, the authors chose to apply differential modulation to avoid channel estimation. This will introduce an SNR-loss and is limited to PSK modulation. The applicability is also limited to channels with short impulse responses, i.e., channels which do not exhibit too severe frequency selectivity. In this paper we consider a coherent OFDM system with channel estimation. We present two algorithms for channel estimation and investigate the performance limits of this interpolation technique for a coherent OFDM system with channel estimation, which offers the prospect of higher-level QAM modulations.

II. SYSTEM MODEL

We apply bit-interleaved coded modulation (BICM). Information bits are convolutionally encoded and randomly interleaved. The resulting code bits are mapped to symbols $d_n(i)$. These are drawn from a QAM/PSK signal constellation. The inverse discrete Fourier transform (IDFT) computes the time-domain signal. After prepending the cyclic prefix the overall OFDM signal in time-domain reads

$$x(k) = \frac{1}{\sqrt{N}} \sum_{i=-\infty}^{\infty} \sum_{\nu=0}^{N-1} d_{\nu}(i) \cdot e^{j2\pi\nu(k-i(N+N_g))/N}, \quad (1)$$

with N subcarriers, N_g symbols for the cyclic prefix, and the OFDM symbol index i . The OFDM signal is received by a linear antenna array consisting of N_r antennas. The impulse response of the frequency- and time selective channel at time instance k and delay $\ell = 0, \dots, L-1$ is denoted by $h_{\ell}(k)$,

the additive noise (AWGN) for the a -th antenna is denoted by $n_a(k) \sim \mathcal{CN}(0, \sigma_n^2)$. The receive signal at the a -th antenna, $0 \leq a \leq N_r - 1$, thus reads

$$y_a(k) = \sum_{\ell=0}^{L-1} h_\ell(k - aD)x(k - \ell) + n_a(k). \quad (2)$$

The spatial antenna distance translates into a reception of the transmit signal via a delayed impulse response whereby the delay between two antennas amounts to D symbols.

To create a virtual non moving antenna, the antenna signals are linearly combined by a Wiener filter. In the following we will refer to a virtual antenna as *point of reception* (POR). We will generate multiple PORs to perform maximum ratio combining to gain diversity. In Sec. V we will elaborate on this idea.

Each POR acts as a diversity branch and is processed by an OFDM receiver, which removes the cyclic prefix, computes the FFT and performs channel estimation (CE). Two algorithms for CE are presented in Sec. IV. The diversity branches are merged by maximum ratio combining (MRC) (cf. Sec. V). After APP-demapping and deinterleaving the Viterbi algorithm (VA) decodes the received code bits.

III. SPATIAL INTERPOLATION

In this section we will repeat the derivation of the interpolator which generates a POR. The original development can be found in [3]. We will assume here that all antenna signals are used to generate a POR. In Sec. V we detail the idea to process two antenna signals at a time to generate multiple PORs.

A virtual non moving antenna is created by a Wiener filter with output

$$\tilde{y}(k) = \sum_{a=0}^{N_r-1} w_a^*(k)y_a(k) = \mathbf{w}^H(k)\mathbf{y}(k). \quad (3)$$

We introduced the Wiener coefficients $w_{k,a}$, the vector definitions $\mathbf{w}(k) = [w_0(k), \dots, w_{N_r-1}(k)]^T$, $\mathbf{y}(k) = [y_0(k), \dots, y_{N_r-1}(k)]^T$ and the complex conjugate $(\cdot)^*$ and Hermitian transpose $(\cdot)^H$. Since (3) represents the signal that we mainly will work with we introduce the equivalent model

$$\tilde{y}(k) = \sum_{\ell=0}^{L-1} \tilde{h}_\ell(k) \cdot x(k - \ell) + \tilde{n}(k) \quad (4)$$

with $\tilde{h}_\ell(k) = \sum_{a=0}^{N_r-1} w_a^*(k)h_\ell(k - aD)$ and $\tilde{n}(k) = \sum_{a=0}^{N_r-1} w_a^*(k)n_a(k)$. The objective function of the Wiener filter is chosen to be $z(k) = \sum_{\ell=0}^{L-1} h_\ell(P)x(k - \ell)$ which means that the transmit signal $x(k)$ seemingly has been received over a channel with constant impulse response $h_\ell(P)$, where P denotes the time index of the impulse response which we desire to interpolate. Please note that $h_\ell(P)$ is the realisation of the channel impulse response $h_\ell(k)$ at epoch $k = P$, hence, it obeys the same statistics. We will refer to P as an *interpolation point*. The Wiener coefficients in (3) are determined by solving the MMSE criterion

$$\mathbb{E} \{ |z(k) - \tilde{y}(k)|^2 \} = \min_{\mathbf{w}(k)}, \quad (5)$$

which is fulfilled by the Wiener-Hopf equation

$$\mathbf{w}(k) = \mathbf{\Phi}^{-1}\boldsymbol{\theta}(k) \quad (6)$$

with autocorrelation (AC) matrix $\mathbf{\Phi} = \mathbb{E}\{\mathbf{y}(k)\mathbf{y}(k)^H\}$ and crosscorrelation (CC) vector $\boldsymbol{\theta}(k) = \mathbb{E}\{\mathbf{y}(k)z^*(k)\}$. For a given channel model the Wiener coefficients can be predetermined. The elements of AC matrix and CC vector are given by

$$[\mathbf{\Phi}]_{a,a'} = \mathbb{E}\{y_a(k)y_{a'}^*(k)\} = \bar{\varphi}_{hh}((a' - a)D) + \sigma_n^2\delta_{a-a'} \quad (7)$$

$$[\boldsymbol{\theta}(k)]_a = \mathbb{E}\{y_a(k)z^*(k)\} = \bar{\varphi}_{hh}(k - aD - P) \quad (8)$$

Here, we introduced the mean autocorrelation function (ACF) of the impulse response for Jakes' channel model as

$$\bar{\varphi}_{hh}(\lambda) = \sum_{\ell=0}^{L-1} \mathbb{E}\{h_\ell(k)h_\ell^*(k + \lambda)\} = J_0(2\pi\lambda\gamma/N). \quad (9)$$

The Bessel function of the first kind is denoted by $J_0(\cdot)$. The variable $\gamma = f_D/\Delta f$ denotes the maximum Doppler frequency f_D normalized to the subcarrier spacing Δf .

To assess the effectiveness of the interpolation approach we compare the variance of the non interpolated impulse response against the interpolated impulse response. Let us define the latter as

$$\sigma_h^2 = \frac{1}{N} \sum_{k=0}^{N-1} \sum_{\ell=0}^{L-1} \mathbb{E} \left\{ \left| \tilde{h}_\ell(k) - \frac{1}{N} \sum_{\mu=0}^{N-1} \tilde{h}_\ell(\mu) \right|^2 \right\}. \quad (10)$$

The former, σ_h^2 , results from replacing $\tilde{h}_\ell(k)$ by $h_\ell(k)$ yielding in terms of (9)

$$\sigma_h^2 = 1 - \frac{1}{N^2} \sum_{\mu=0}^{N-1} \sum_{\mu'=0}^{N-1} \bar{\varphi}_{hh}(\mu - \mu'). \quad (11)$$

To evaluate (10) let us define the $(N_r \times N_r)$ matrix $\boldsymbol{\Theta}(\lambda)$ with elements $[\boldsymbol{\Theta}(\lambda)]_{m,n} = \bar{\varphi}_{hh}(\lambda - (m - n)D)$. The variance of the interpolated channel impulse response then reads

$$\sigma_h^2 = \sum_{k=0}^{N-1} \frac{\mathbf{w}^H(k)\boldsymbol{\Theta}(0)\mathbf{w}(k)}{N} - \sum_{k,k'=0}^{N-1} \frac{\mathbf{w}(k)^H\boldsymbol{\Theta}(k-k')\mathbf{w}(k')}{N^2}. \quad (12)$$

The variance of the non interpolated impulse response (11) depends only on two parameters, i.e., the number of subcarriers and the maximum Doppler frequency. The dependencies of (12) include on top of that the noise variance, the antenna distance and the interpolation point.

In a practical system we are forced to fix the antenna distance. Ignoring this fact for the moment we will exemplify the minimal variances σ_h^2 , one can expect from the interpolation technique, if the antenna distance is chosen such that the channel's variance becomes minimal.

We have illustrated in Fig. 1 the ratio of the variance of the interpolated channel to the non interpolated channel for two different signal-to-noise ratios and different maximum Doppler frequencies. We see that the minima are dependent on the noise level, i.e., the smaller the noise, the smaller the

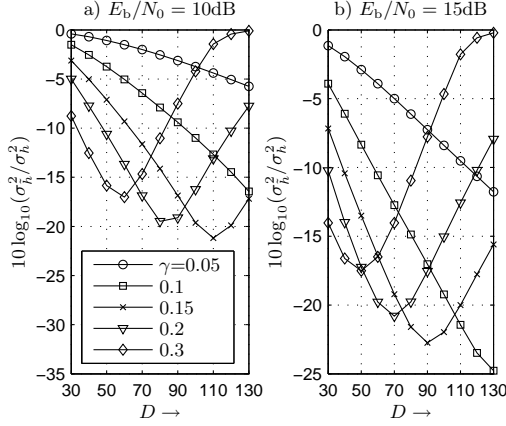


Fig. 1. Ratio of interpolated channel variance to the non-interpolated channel variance, QPSK, $N_r = 2$

minimal variance against the single antenna case. We can also see that a large Doppler frequency demands a small antenna distance, since only then the antenna correlations are large enough for a satisfying interpolation outcome and, eventually, for a small bit error rate (BER). On the contrary, for small Doppler frequencies it is advantageous to have a larger antenna spacing. This can not be seen from the variance ratio, but will be evidenced on the basis of BER measurements in the simulation results. In practice one has to find a compromise.

A. Correlation and variances in frequency domain

In this section we summarize correlation functions and variances which are necessary for the application of the subsequent channel estimators.

At the receiver the discrete Fourier transform (DFT) of the linearly combined signal (4) reads

$$\tilde{r}_n(i) = \frac{1}{\sqrt{N}} \sum_{\mu=0}^{N-1} \tilde{y}(\mu + i(N + N_g)) e^{-j2\pi\mu n/N}. \quad (13)$$

We aim at separating the transmitted symbol $d_n(i)$ from the ICI and the noise term in (13). Substituting (4) in (13) then yields after a few steps

$$\tilde{r}_n(i) = \sum_{\nu=0}^{N-1} \sum_{\ell=0}^{L-1} d_\nu(i) H_\ell(i, \nu - n) e^{-j2\pi\nu\ell/N} + \tilde{\eta}_n(i) \quad (14)$$

with

$$H_\ell(i, \nu - n) = \frac{1}{N} \sum_{\mu=0}^{N-1} \tilde{h}_\ell(\mu + i(N + N_g)) e^{j2\pi\mu(\nu - n)/N} \quad (15)$$

and $\tilde{\eta}_n(i)$ being the DFT of $\tilde{\eta}(k)$. We can now separate the useful signal from ICI and noise

$$\tilde{r}_n(i) = \tilde{H}_n(i) \cdot d_n(i) + \zeta_n(i) + \tilde{\eta}_n(i) \quad (16)$$

with

$$\tilde{H}_n(i) = \sum_{\ell=0}^{L-1} H_\ell(i, 0) e^{-j2\pi n\ell/N}, \quad (17)$$

and the ICI term

$$\zeta_n(i) = \sum_{\substack{\nu=0 \\ \nu \neq n}}^{N-1} \sum_{\ell=0}^{L-1} d_\nu(i) H_\ell(i, \nu - n) \cdot e^{-j2\pi\nu\ell/N}. \quad (18)$$

The ACF of $\tilde{H}_n(i)$ reads

$$E\{\tilde{H}_n(i) \tilde{H}_{n+\Delta n}^*(i + \Delta i)\} = \theta_f(\Delta n) \cdot \theta_t(\Delta i) \quad (19)$$

with the partial correlation functions

$$\theta_f(\Delta n) = \sum_{\ell=0}^{L-1} \sigma_\ell^2 e^{j2\pi\ell\Delta n/N}, \quad (20)$$

$$\theta_t(\Delta i) = \sum_{k, k'=0}^{N-1} \frac{\mathbf{w}(k)^H \Theta(k - k' - \Delta i(N + N_g)) \mathbf{w}(k')}{N^2}. \quad (21)$$

The ICI-power is identical to (12)

$$\sigma_\zeta^2 = E\{|\zeta_n(i)|^2\} = \sigma_h^2, \quad (22)$$

and the noise power in frequency domain is given by

$$\sigma_{\tilde{\eta}}^2 = E\{|\tilde{\eta}_n(i)|^2\} = \frac{1}{N} \sum_{k=0}^{N-1} \|\mathbf{w}(k)\|^2 \sigma_n^2. \quad (23)$$

IV. CHANNEL ESTIMATION

We describe two algorithms for channel estimation. Immediately to follow is the least square approach, which is based on pilot symbols in each OFDM symbol spaced in frequency at a distance of Δ_f symbols. Although the large amount of training reduces the useful data-rate we are able to cope with large Doppler frequencies. Speaking of data-rate leads us subsequently to our second, minimum mean square error approach which relies on a scattered pilot-scheme. Here, we space pilot-symbols additionally in time at a distance of Δ_t symbols. The channel for OFDM symbols which are not carrying any pilot symbols at all can then be interpolated based on neighboring pilots. On the one hand the data-rate is increased, but on the other hand we still have to adhere to the sampling theorem. We can already suspect that the interpolation technique will be beneficial only if the pilot spacing in time direction is close to the critical sampling frequency of twice the maximum Doppler frequency.

A. Least Square Channel Estimation

The received signal in frequency domain is given by (16). We assume that N_p equidistant pilot symbol are distributed in frequency direction with distance Δ_f . Hence, dividing by the corresponding pilot symbol yields an estimate of the channel coefficient at these positions

$$\tilde{H}_{n\Delta_f}^{\text{LS}}(i) = \frac{\tilde{r}_{n\Delta_f}(i)}{d_{n\Delta_f}(i)} = \tilde{H}_{n\Delta_f}(i) + \frac{\zeta_{n\Delta_f}(i) + \tilde{\eta}_{n\Delta_f}(i)}{d_{n\Delta_f}(i)}. \quad (24)$$

An estimate of the impulse response follows directly from these channel coefficients using the IDFT

$$\hat{h}_\ell^{\text{LS}}(i) = \frac{1}{N_p} \sum_{n=0}^{N_p-1} \tilde{H}_{n\Delta_f}(i) e^{-j2\pi n\Delta_f\ell/N}. \quad (25)$$

This approach exploits the fact that the channel transfer function is usually oversampled, i.e., the number of subcarriers

is much larger than the cyclic prefix and the impulse response. Assuming that $N_p = L$ yields

$$\hat{h}_\ell^{\text{LS}}(i) = H_\ell(i, 0) + \eta_\ell^{\text{LS}}(i) \quad (26)$$

with $\eta_\ell^{\text{LS}}(i) = \frac{1}{N_p} \sum_{n=0}^{N_p-1} \frac{\zeta_n \Delta_f(i) + \tilde{\eta}_n \Delta_f(i)}{d_n \Delta_f(i)} e^{-j2\pi n \Delta_f \ell / N}$. It is seen from (17) that $H_\ell(i, 0)$ in (26) equals the mean channel impulse response during one OFDM-symbol. Hence, the DFT of (26) produces a noisy estimate of the effective channel transfer function (17)

$$\hat{H}_n^{\text{LS}}(i) = \sum_{\ell=0}^{N_p-1} \hat{h}_\ell^{\text{LS}}(i) e^{j2\pi \ell n / N} . \quad (27)$$

The LS channel estimator has the advantage of an easy implementation, since the estimation process only involves one IDFT and one DFT. Those can be conveniently realized by their fast Fourier counterparts. Additionally the channel can be estimated without any knowledge about the channel's power delay profile. On the downside we have the reduction of the useful data rate, since every OFDM symbol needs to carry pilot symbols. This leads to the following MMSE channel estimator.

B. Minimum Mean Square Energy Channel Estimation

The MMSE channel estimator allows us to exploit a scattered pilot scheme, i.e., some OFDM symbols are completely free of training data. Hence, we have need of an estimator which can interpolate the channel transfer function not only in frequency direction but also in time direction. With a slight abuse of notation we define the channel coefficient at the ν -th subcarrier in the μ -th OFDM symbol as

$$\check{H}_\nu^{\text{LS}}(\mu) = \frac{\tilde{r}_\nu(\mu)}{d_\nu(\mu)} = \check{H}_\nu(\mu) + \frac{\zeta_\nu(\mu) + \tilde{\eta}_\nu(\mu)}{d_\nu(\mu)} . \quad (28)$$

Since we are considering a rectangular pilot grid, ν and μ are multiples of Δ_f and Δ_t , respectively.

The Wiener coefficients for CE, $\mathbf{w}_n^{\text{MMSE}}(i)$, follow by solving

$$\text{E} \left\{ \left| \check{H}_n(i) - (\mathbf{w}_n^{\text{MMSE}}(i))^H \check{\mathbf{H}}_n^{\text{LS}}(i) \right|^2 \right\} = \min_{\mathbf{w}_n^{\text{MMSE}}(i)} . \quad (29)$$

We define the vector $\check{\mathbf{H}}_n^{\text{LS}}(i)$ as

$$\check{\mathbf{H}}_n^{\text{LS}}(i) = \left[\check{H}_{\nu_0}^{\text{LS}}(\mu_0), \check{H}_{\nu_1}^{\text{LS}}(\mu_1), \dots, \check{H}_{\nu_{N_w-1}}^{\text{LS}}(\mu_{N_w-1}) \right]^T . \quad (30)$$

It carries LS channel estimates closest to the channel coefficient $\check{H}_n(i)$. To find these we follow the balanced design rule of [5]. In short, this rule ensures that pilots are chosen, which are lying in a direction of large correlation. For example, if the channel is lowly frequency-selective, but highly time-selective, mainly pilots in frequency direction will be chosen. We denote by $\check{H}_{\nu_0}^{\text{LS}}(\mu_0)$ the channel coefficient at pilot position (ν_0, μ_0) which is closest to (n, i) in terms of the balanced design. Consequently, $\check{H}_{\nu_1}^{\text{LS}}(\mu_1)$ is the second closest, et cetera. Please note, that the selection of the pilots depends on (n, i) . We have omitted this detail in (30) to avoid cluttering notation. Eq. (29) is solved by

$$\mathbf{w}_n^{\text{MMSE}}(i) = (\check{\Phi}_n^{\text{LS}}(i))^{-1} \check{\theta}_n^{\text{LS}}(i) \quad (31)$$

with AC-matrix $\check{\Phi}_n^{\text{LS}}(i)$ and CC-vector $\check{\theta}_n^{\text{LS}}(i)$ given by

$$\check{\Phi}_n^{\text{LS}}(i) = \text{E} \left\{ \check{\mathbf{H}}_n^{\text{LS}}(i) (\check{\mathbf{H}}_n^{\text{LS}}(i))^H \right\}, \quad \check{\theta}_n^{\text{LS}}(i) = \text{E} \left\{ \check{\mathbf{H}}_n^{\text{LS}}(i) \check{H}_n^*(i) \right\} \quad (32)$$

Consequently, $\mathbf{w}_n^{\text{MMSE}}(i)$ is a $(N_w \times 1)$ -vector, i.e., N_w pilot symbols are used to interpolate the channel coefficient at the n -th subcarrier in the i -th OFDM symbol. The elements of $\check{\Phi}_n^{\text{LS}}(i)$ and $\check{\theta}_n^{\text{LS}}(i)$ are given by

$$\left[\check{\Phi}_n^{\text{LS}}(i) \right]_{x,y} = \theta_f(\nu_x - \nu_y) \cdot \theta_t(\mu_x - \mu_y) + \sigma_{\eta^{\text{LS}}}^2(x - y) \quad (33)$$

$$\left[\check{\theta}_n^{\text{LS}}(i) \right]_x = \theta_f(\nu_x - n) \cdot \theta_t(\mu_x - i) \quad (34)$$

$$\sigma_{\eta^{\text{LS}}}^2(x - y) = \frac{\delta_{x-y}}{|d_{\nu_x}(\mu_x)|^2} \left(\sigma_h^2 + \frac{\sigma_n^2}{N} \sum_{k=0}^{N-1} \|\mathbf{w}(k)\|^2 \right) \quad (35)$$

The MMSE channel estimate is finally given by

$$\hat{H}_n^{\text{MMSE}}(i) = (\mathbf{w}_n^{\text{MMSE}}(i))^H \check{\mathbf{H}}_n^{\text{LS}}(i) . \quad (36)$$

V. MAXIMUM RATIO COMBINING RECEIVER

Based on (4) it is possible to perform demodulation followed by decoding. To this end, all antennas of the linear antenna array are used to generate the POR. However, the more antennas are employed the less the outer antennas are correlated. Hence, linearly combining these signals is actually an averaging process reducing the effective SNR. The authors of [4] propose to compute several PORs from a linear antenna array using all available N_r antennas. We present a variant of this idea and propose to compute $N_r - 1$ PORs. These PORs run between all pairs of neighboring antennas. As a result we are avoiding unnecessary signal correlations which is beneficial for the subsequent maximum ratio combining. Let us assume that the p -th POR lies between the p -th and the $(p + 1)$ -th antenna with $0 \leq p \leq N_r - 2$. The received signal in frequency domain at the p -th POR reads

$$\tilde{r}_{n,p}(i) = \check{H}_{n,p}(i) \cdot d_n(i) + \zeta_{n,p}(i) + \tilde{\eta}_{n,p}(i) \quad (37)$$

Maximum ratio combining of all PORs yields

$$\rho_n(i) = \frac{\sum_{p=0}^{N_r-2} \left(\hat{H}_{n,p}^{\text{LS/MMSE}}(i) \right)^* \tilde{r}_{n,p}(i)}{\sum_{p=0}^{N_r-2} |\hat{H}_{n,p}^{\text{LS/MMSE}}(i)|^2} \quad (38)$$

If we assume that the channel estimates are perfect, we can approximate (38) by an equivalent AWGN channel

$$\rho_n(i) \approx d_n(i) + \eta_n^{(\rho)}(i) . \quad (39)$$

The noise term $\eta_n^{(\rho)}(i)$ is assumed to be zero-mean AWGN with variance

$$\text{E} \left\{ \left| \eta_n^{(\rho)}(i) \right|^2 \right\} = \frac{\sigma_\zeta^2 + \sigma_\eta^2}{\sum_{p=0}^{N_r-2} |\hat{H}_{n,p}^{\text{LS/MMSE}}(i)|^2} . \quad (40)$$

Please note that the variance of $\eta_n^{(\rho)}(i)$ differs with subcarrier index n and OFDM symbol index i . Based on (39) we perform APP-demodulation followed by deinterleaving and VA decoding.

VI. SIMULATION RESULTS

We present results for the WSSUS channel model with Jakes' Doppler spectrum and uniformly distributed power delay profile of length L . For the OFDM system we chose HIPERLAN parameters, i.e., $N = 64$ subcarriers and $N_g = 16$ guard taps. The common $(133, 171)_8$ convolutional code with a block length of 10^4 information bits was applied. The interpolation point P was chosen such that (10) yielded a minimum for a fixed antenna distance.

a) Least Square Channel Estimation: In Fig. 2 BER measurements are shown for a small Doppler frequency ($\gamma = 0.05$) and strong frequency selectivity ($L = 10$). Based on Fig. 1 two different antenna delays ($D = 64, 128$) were examined. Comparing the two and eight antenna case reveals that the antenna spacing has a more severe effect on the eight antenna case. All modulation forms are improving if the number of antennas as well as their distance is increased. A diversity effect is visible in both cases. It is also evident that differential QPSK suffers extremely due to the frequency selective conditions. The superiority of the coherent over the noncoherent approach is obvious for QPSK and 16QAM.

Let us turn to the fast Doppler case in Fig. 3. Unlike the small Doppler case we have to ensure a narrow antenna spacing. Otherwise the signals will be only loosely correlated, resulting in an unsatisfying BER floor. Please note that the single antenna case with perfect CSI ends in an error floor. Like in a practical OFDM receiver we equalized the received symbols on the basis of the mean channel impulse response, hence, ICI leads to an error floor.

b) MMSE Channel Estimation: Fig. 4 compares the performance of the interpolation approach against single antenna reception for a scattered pilot scheme. The cut-off frequency for critical sampling the channel lies at $\gamma \approx 0.094$. Closing in on this frequency the BER of single antenna reception soon deteriorates, whereas the interpolating receiver still yields satisfying results.

VII. CONCLUSION

We presented two channel estimators for spatially interpolated coherent OFDM and demonstrated its higher performance against the noncoherent counterpart. We have seen that a smaller antenna spacing not necessarily improves the resulting BER performance. In fact, only large Doppler benefits from a narrow antenna spacing, whereas small Doppler frequency are better dealt with by larger antenna spacings.

REFERENCES

- [1] W. G. Jeon, K. H. Chang, "An equalization technique for orthogonal frequency-division multiplexing systems in time-variant multipath channels", *IEEE Trans. Comm.*, Vol. 47, pp. 27-32, Jan. 1999
- [2] Y. Mostofi, D. C. Cox, "ICI Mitigation for Pilot-Aided OFDM Mobile Systems", *IEEE Trans. on Wireless Comm.*, Vol. 4, No. 2, pp. 765-774, March 2005
- [3] H. Takayanagi, M. Okada, H. Yamamoto, "Novel Fast Fading Compensator for OFDM using Space Diversity with Space-Domain Interpolator", *54th VTC 2001 (Fall)*, Vol. 1, pp. 479-483
- [4] K. Kitanosono, T. Taniguchi, M. Okada, H. Yamamoto, "Performance of OFDM Diversity Receiver with Array Antenna Assisted Doppler Spread Compensator", *9th International OFDM-Workshop (InOWo '04)*, Proceedings, pp. 119-122

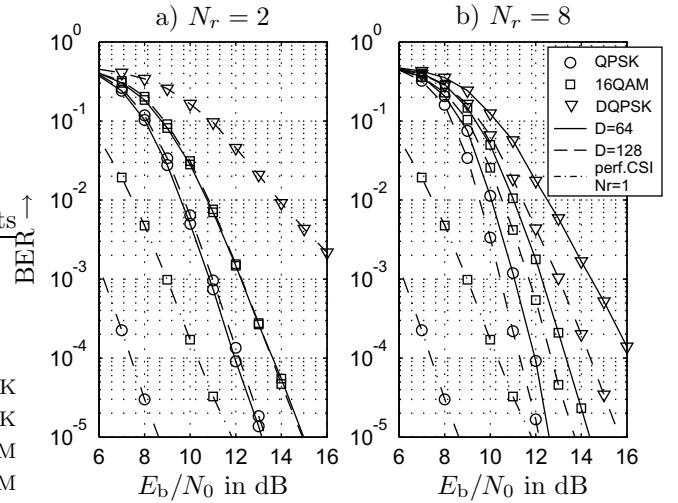


Fig. 2. Parameters: $\gamma = 0.05$, $L = 10$, pilot spacing $\Delta_f = 4$

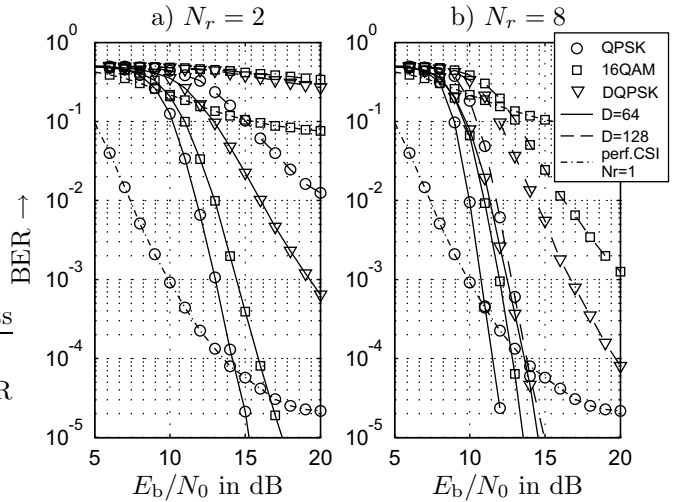


Fig. 3. Parameters: maximum Doppler frequency $\gamma = 0.3$, $L = 10$, pilot spacing $\Delta_f = 4$

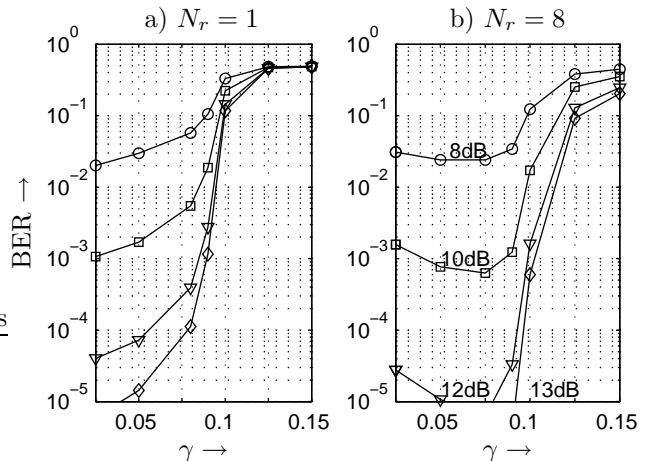


Fig. 4. MMSE channel estimation for scattered pilot scheme with $\Delta_t = \Delta_f = 4$, 16QAM, $N_w = 20$, $D = 128$

- [5] P. Höher, S. Kaiser, P. Robertsson, "Two-Dimensional Pilot-Symbol-Aided Channel Estimation By Wiener Filtering", *ICASSP 1997*